THE JOURNAL OF BIOLOGICAL CHEMISTRY VOL. 288, NO. 19, pp. 13397–13409, May 10, 2013
Published in the U.S.A.

Myristate-derived d16:0 Sphingolipids Constitute a Cardiac Sphingolipid Pool with Distinct Synthetic Routes and Functional Properties*[S]

Received for publication, October 15, 2012, and in revised form, March 21, 2013 Published, JBC Papers in Press, March 25, 2013, DOI 10.1074/jbc.M112.428185

Sarah Brice Russo[‡], Rotem Tidhar[§], Anthony H. Futerman[§1], and L. Ashley Cowart[‡¶2]

From the [‡]Department of Biochemistry and Molecular Biology, Medical University of South Carolina, Charleston, South Carolina 29403, the [§]Department of Biological Chemistry, Weizmann Institute of Science, Rehovot 76100, Israel, and the [¶]Ralph H. Johnson Veterans Affairs Medical Center, Charleston, South Carolina 29403

Background: Myristate is a novel potential substrate for sphingoid base synthesis.
Results: Myocardial sphingoid base synthesis utilizes myristate; these sphingolipids are functionally non-redundant with canonical sphingoid bases.
Conclusion: d16:0 and d16:1 sphingolipids constitute an appreciable proportion of cardiac dihydrosphingosine and dihydroceramide, with distinct biological roles.
Significance: This pool of sphingolipids may play a heretofore unsuspected role in myocardial pathology or protection.

The enzyme serine palmitoyltransferase (SPT) catalyzes the formation of the sphingoid base "backbone" from which all sphingolipids are derived. Previous studies have shown that inhibition of SPT ameliorates pathological cardiac outcomes in models of lipid overload, but the metabolites responsible for these phenotypes remain unidentified. Recent *in vitro* studies have shown that incorporation of the novel subunit SPTLC3 broadens the substrate specificity of SPT, allowing utilization of myristoyl-coenzyme A (CoA) in addition to its canonical substrate palmitoyl-CoA. However, the relevance of these findings *in vivo* has yet to be determined. The present study sought to determine whether myristate-derived d16 sphingolipids are represented among myocardial sphingolipids and, if so, whether their function and metabolic routes were distinct from those of palmitate-derived d18 sphingolipids. Data showed that d16:0 sphingoid bases occurred in more than one-third of total dihydrosphingosine and dihydroceramides in myocardium, and a diet high in saturated fat promoted their *de novo* production. Intriguingly, d16-ceramides demonstrated highly limited *N*-acyl chain diversity, and *in vitro* enzyme activity assays showed that these bases were utilized preferentially to canonical bases by CerS1. Functional differences between myristate- and palmitate-derived sphingolipids were observed in that, unlike d18 sphingolipids and SPTLC2, d16 sphingolipids and SPTLC3 did not appear to contribute to myristate-induced autophagy, whereas only d16 sphingolipids promoted cell death and cleavage of poly(ADP-ribose) polymerase in cardiomyocytes. Thus, these results reveal a previously unappreciated component of cardiac sphingolipids with functional differences from canonical sphingolipids.

Sphingolipids constitute a class of structural and signaling lipids that regulate numerous processes in the cell, including inflammation, proliferation, autophagy, and cell death (reviewed in Refs. 1 and 2). Although, as a class, sphingolipids are chemically diverse, all sphingolipids are ultimately derived from the sphingoid base dihydrosphingosine (DHS,[3] also known as sphinganine), which arises from the condensation of a fatty acyl-coenzyme A (CoA) to an amino acid (usually palmitoyl-CoA and serine, respectively) by the enzyme serine palmitoyltransferase (SPT) (reviewed in Refs. 3–5). This reaction forms the transient product 3-ketodihydrosphingosine, which undergoes rapid reduction to DHS. DHS serves as substrate for ceramide biosynthesis, and thus, its production constitutes a key step for all sphingolipid synthesis.

Because production of sphingoid bases by SPT is the rate-limiting step of *d*, *u* sphingolipid synthesis, the structure, enzymology, and regulation of this enzyme are of considerable interest, particularly in tissues that are subject to sphingolipid-mediated pathology, including the heart. The functional SPT enzyme occurs as a complex composed of one or more heterodimers (6). Each of these heterodimers contains one non-catalytic SPTLC1 subunit, which anchors the complex to the membrane, and one catalytic SPTLC2 or SPTLC3 subunit. Most studies have focused on SPTLC2 and its product, which derives from palmitoyl-CoA (reviewed in Ref. 4). However,

* This work was supported, in whole or in part, by National Institutes of Health (NIH), NIDDK, Grant F30DK092125 (to S.B.R.); NIH Grant P30 CA138313 (Lipidomics Shared Resource, Hollings Cancer Center, Medical University of South Carolina (MUSC)); NIH Grant P20 RR017677 (Lipidomics Core in the South Carolina Lipidomics and Pathobiology Centers of Biomedical Research Excellence (COBRE), Department of Biochemistry, MUSC); and the NIH COBRE in Lipidomics and Pathobiology at MUSC (to L. A. C.). This work was also supported by a Merit Award from the Department of Veterans Affairs (to L. A. C.).

[S] This article contains supplemental Fig. 1.

[1] The Joseph Meyerhoff Professor of Biochemistry at the Weizmann Institute of Science.

[2] To whom correspondence should be addressed: Dept. of Biochemistry and Molecular Biology, Ralph H. Johnson Veterans Affairs Medical Center, Medical University of South Carolina, 173 Ashley Ave., MSC509, Charleston, SC 29403. Tel.: 843-792-4321; Fax: 843-792-0283; E-mail: cowartl@musc.edu.

[3] The abbreviations used are: DHS, dihydrosphingosine; SPT, serine palmitoyltransferase; DHC, dihydroceramide; Cer, ceramide; CerS, (dihydro)ceramide synthase; Des1, dihydroceramide desaturase 1; PARP, poly(ADP-ribose) polymerase; MTT, 3-(4,5-dimethylthiazol-2-yl)-2,5-diphenyltetrazolium bromide; qRT-PCR, quantitative RT-PCR.

recent studies have indicated that incorporation of other subunits, such as SPTLC3 and novel putative small subunits, into the SPT complex can shift the acyl-CoA substrate preferences of the enzyme (7, 8). In particular, the presence of SPTLC3 in the SPT enzyme complex promoted utilization of myristoyl-CoA, resulting in production of a d16:0 sphingoid base (7). This alteration of substrate preferences could thus increase the diversity of cellular sphingoid bases and possibly generate lipids with distinct functions. However, to date, no studies have attempted to determine the relative abundance of d16:0 sphingoid bases in tissues that highly express SPTLC3. Moreover, it remains unknown whether these bases are routed through similar sphingolipid metabolic pathways to those of palmitoyl-CoA-derived d18:0 bases. Finally, and perhaps most importantly, it has not been determined whether this previously unappreciated pool of lipids participates in the same pathways as d18:0 sphingoid bases and their metabolites.

The present study addresses the enzymology of SPTLC3 in the myocardium, the metabolism of myristate-derived sphingolipids both basally and in response to fatty acid overload, and the potential contributions of these lipids to sphingolipid-dependent cardiomyocyte autophagy in lipid overload. In brief, it was found that d16:0-DHS and its downstream products constitute a previously unconsidered proportion of the myocardial sphingolipidome. A diet high in saturated fat stimulated their production, which was mediated by defined metabolic routes. In cultured cardiomyocytes, exposure to myristate, but not palmitate, increased expression of SPTLC3 and production of d16:0-DHS and its derivatives. SPTLC3 and its d16:0 products were implicated in promoting cleavage of poly(ADP-ribose) polymerase (PARP), a marker of apoptosis, but not in induction of pathological sphingolipid-dependent autophagy by myristate oversupply, suggesting different intracellular roles for myristate- and palmitate-derived sphingoid bases and their derivatives in the heart.

MATERIALS AND METHODS

l d —In all studies, C57BL/6 male mice (Jackson Laboratory, Bar Harbor, ME) were given water and chow *a* . For SPT enzyme assays, mice were fed standard laboratory chow. For diet studies, high fat diets (60% of calories from fat) and an isocaloric low fat diet (16.8% of calories from fat, TD.08810) were purchased from Harlan Laboratories, Inc. (Indianapolis, IN). High fat diets were based on lard (TD.06414) or milk fat (TD.09766). All components of the diets were identical except for substitution of lard or anhydrous milk fat for the low glycemic index starch of the control diet. For the high fat diet studies, 12 8-week-old mice were placed in each group and maintained on the diets for a total of 8, 16, or 18 weeks. At the 8- and 16-week time points, whole hearts were isolated, snap-frozen, and pulverized to provide tissue aliquots for analysis. At 18 weeks, the left ventricle of each heart was isolated, snap-frozen, and pulverized to provide tissue aliquots for analysis.

d l x , x , d x—Microsomal SPT was assayed essentially as described previously (9). For each assay, nine 12-week-old male C57Bl/6J mice were sacrificed. Hearts were rinsed thoroughly in PBS, finely minced in sonication buffer (25 mM Tris, pH 7.4; 5 mM EDTA; 1 mM phenylmethylsulfonyl fluoride; 20 μg/ml chymotrypsin, leupeptin, antipain, and pepstatin), pooled, and disrupted by probe sonication. The homogenate was centrifuged for 5 min at 1000 $\times f$, and the supernatant was then subjected to centrifugation at 100,000 $\times f$ for 1 h. The resulting pellet was resuspended in a small volume of 25 mM Tris, pH 7.4, containing 30% glycerol. Protein concentration was measured using the Micro BCA protein assay kit (Fisher). For each replicate, 100 μg of microsomal protein was incubated at 37 °C for 20 min in the presence of 100 mM HEPES, pH 8.3, 5 mM dithiothreitol, 50 μM pyridoxal-5′-phosphate, 5 mM [^{3}H]serine (30,000 cpm/nmol), and myristoyl-CoA or palmitoyl-CoA, as indicated. At the end of the assay, reactions were stopped by the addition of 1.5 ml of $CHCL_3$/CH_3OH (1:2). Phase separation was induced by the addition of 2 ml of 0.5 N NH_4OH and 1 ml of $CHCl_3$. The aqueous phase was removed, and the organic phase was washed twice with water and dried. [^{3}H]incorporation into the sample was counted by liquid scintillation. Assays were performed three times, with 3–4 replicates/point/assay. Analyses of enzyme kinetics were performed using the SigmaPlot version 10.0 enzyme kinetics analysis module (Systat Software, Inc., San Jose, CA). $_{/}$ values remained constant between assays; however, absolute $_{max}$ values varied between assays. To report the most robust possible activity data, data from each assay were calculated as -fold change over the velocity obtained at 50 μM palmitoyl-CoA in that assay. The resulting data were aggregated from all assays and are presented as relative enzyme activity (Fig. 3). $_{max}$ values are reported in units of relative activity; the absolute values are estimated to be 19.56 pmol/mg protein/min for myristoyl-CoA and 19.46 pmol/mg of protein/min for palmitoyl-CoA, based on a representative assay.

To verify that the assay conditions themselves did not result in a loss of substrate specificity, SPT was assayed in microsomes derived from liver. In our hands, SPTLC3 expression in the livers of 8-week-old mice was 19.5% of that observed in heart, and the rate of utilization of myristoyl-CoA by liver microsomes was only 56% of that observed with palmitoyl-CoA (data not shown). These findings indicate that the assay conditions themselves did not promote utilization of myristoyl-CoA by the SPT enzyme.

d , , x , x d—Adult feline cardiomyocytes were isolated using a hanging heart preparation with enzymatic digestion, per Institutional Animal Care and Use Committee approval, and cultured as previously described (10). Cardiomyocytes were plated on laminin-coated dishes at an initial cell density of 7.5 $\times$ 10^4 cells/ml.

H9c2 immortalized cardiomyocytes were obtained from ATCC and maintained in Dulbecco's modified Eagle's medium supplemented with 10% fetal bovine serum, per ATCC instructions. Cells were utilized for experiments only up through passage nine.

x , f , d —For most studies, concentrated free fatty acid stock solutions were prepared fresh by supplementing media with 2% fatty acid-free BSA and either 1.5 mM myristate, 2.0 mM palmitate, or vehicle. Solutions were sonicated briefly, incubated for 15 min at 55 °C, and cooled to 37 °C. Cells were incubated in a final concentration of 0.75 mM myristate or 1.0 mM palmitate for 16 h. For

studies employing siRNA transfection, cells were treated instead with 0.1 mM myristate, prepared as above, to minimize lipotoxicity. For sphingoid base treatments, culture medium was supplemented with a final concentration of 2.5 μM d18:0-DHS or d16:0-DHS (Matreya, Pleasant Gap, PA) or an equivalent volume of ethanol. Cells were maintained in DHS for 3 h and then harvested. Experiments were performed 2–3 times in triplicate.

3-(4,5- l d x y -2-x)-2,5- d x d y -

l d (I) *x*—After treatment with sphingoid bases, as indicated, H9c2 cells were treated with MTT (Invitrogen) for 1.5 h. MTT reduction, an indicator of metabolic activity, was then assessed per the manufacturer's instructions. The assay was performed twice, with at least three replicates per point.

M d —Using Lipofectamine 2000 (Invitrogen) according to the manufacturer's instructions, cardiomyocytes were transfected with siRNA oligonucleotides. Custom feline siRNAs directed against SPTLC2, SPTLC3, and CerS1 were purchased from Invitrogen. AllStars negative control siRNA was obtained from Qiagen. Cells were transfected for 24 h prior to supplementation with BSA or 0.1 myristate, as described above, and maintained in culture for 16 h.

d f—Cells were washed twice with sterile filtered cold PBS and lysed in buffer containing 20 mM Tris (pH 7.5), 150 mM NaCl, 1 mM EDTA, 1 mM EGTA, 2.5 mM sodium pyrophosphate, 1 mM β-D-glycerophosphate, 1 mM sodium orthovanadate, 1% Triton X-100, and Complete Mini protease inhibitor (Roche Applied Science). Cells were disrupted by freeze-thaw and incubated on ice for 10 min; insoluble material was then removed by centrifugation at 4 °C. Protein concentration was measured using a Micro BCA protein assay kit (Fisher), and equal amounts of protein were loaded for SDS-PAGE and immunoblotted as described previously (11). Membranes were incubated with antibodies against PARP (Santa Cruz Biotechnology, Inc., Santa Cruz, CA), GFP (Cell Signaling Technology), Atg7 (Cell Signaling Technology), or actin (Sigma-Aldrich) and with anti-rabbit secondary antibody (Cell Signaling). Proteins were visualized by enhanced chemiluminescence. Quantification of images was performed using ImageJ software (National Institutes of Health, Bethesda, MD). Results are presented as mean ± S.E. and shown with a representative immunoblot image.

M d -l d x—Total RNA was isolated with TRIzol (Invitrogen), according to the manufacturer's protocol, and cDNA was synthesized using SuperScript III (Invitrogen). Quantitative real-time PCR was performed using SYBR Green reagent (Bio-Rad) as described previously (11). Results were normalized to GAPDH. Primers for SPTLC1, SPTLC2, SPTLC3, ATG7, and GAPDH were obtained from SABiosciences (Frederick, MD). Beclin 1 primers were ordered from Integrated DNA Technologies (Coralville, IA).

l x—Lipidomic profiling was performed by LC/MS by the Lipidomics Core Facility at the Medical University of South Carolina, as described previously (12). For measurements of hearts from diet studies, aliquots from all surviving mice were analyzed. Analyses were performed on samples containing equal amounts of protein, as determined using the Micro BCA protein assay kit (Fisher), and results were normalized to protein.

(x) d x d x—For (dihydro)ceramide synthase (CerS) assays, human embryonic kidney (HEK) 293T cells were cultured in Dulbecco's modified Eagle's medium supplemented with 10% fetal calf serum, 100 μg/ml streptomycin, and 100 IU/ml penicillin and transfected as described previously (13). Cells were transfected with either the empty pCMV vector or vectors containing CerS. Thirty-six h after transfection, cells were washed twice with PBS and homogenized in 20 mM HEPES-KOH, pH 7.2, 25 mM KCl, 250 mM sucrose, 2 mM $MgCl_2$, and a protease inhibitor mixture (Sigma), and assays were performed essentially as described previously (13). To test substrate specificity, activities were measured with either d16:0-DHS or d18:0-DHS and ^{14}C-labeled palmitoyl(C16:0)-CoA, oleoyl(C18:1)-CoA, steroyl(C18:0)-CoA, and lignoceroyl(C24:0)-CoA (all ^{14}C-labeled lipids were from ARC), in accordance with the acyl-CoA specificities of each CerS (14). The assay was performed twice, with at least 4 replicates/substrate combination/isoform. Although each CerS isoform was tested with all of the fatty acyl-CoA species listed above, results for each isoform are shown only for the acyl-CoA providing maximal activity. Data are not shown for CerS3 because activity did not exceed that observed with empty vector.

x d—Data are expressed as mean ± S.E. and were analyzed by two-tailed, unpaired Student's test or two-way analysis of variance, as appropriate. < 0.05 was considered statistically significant. Enzyme kinetic analyses were performed as described above.

x—Animal protocols were in accordance with National Institutes of Health guidelines (25) and have been approved by the Institutional Animal Care and Use Committee at the Medical University of South Carolina.

RESULTS

16:0 16:1 f d I x f d—Initial reports demonstrated that overexpression of SPTLC3 increased the production of unusual myristate-derived sphingoid bases (denoted as d16:0 or d16:1 upon desaturation to sphingosine, henceforth indicated as "d16" when discussed collectively), which derive 14 carbons from the acyl chain of myristoyl-CoA and the remaining two from serine (7). However, it was not determined whether d16:0-DHS and its derivatives constituted a significant proportion of total DHS, dihydroceramide, ceramide, and sphingosine (referred to as "simple sphingolipids" henceforth, consistent with use of the term previously (5, 15–18)) . Intriguingly, SPTLC3 mRNA was shown to be richly expressed in the heart, based on a human cDNA panel (19). Consistent with these findings, SPTLC3 was found to be highly expressed in murine myocardium (Fig. 1). Indeed, SPTLC3 mRNA was much more abundant in the heart than in skeletal muscle, both absolutely and relative to expression of SPTLC1, which dimerizes with the catalytic subunits to form a functional complex (6). Because sphingolipid profiles have been shown to play an important role in cardiac pathology in diabetes (20), we examined whether SPTLC3 expression in the heart was associ-

ated with production of significant levels of non-canonical d16 sphingolipids.

To test this, LC-MS analysis was performed on murine myocardial tissue homogenates, and d16, d20 (derived from stearoyl-CoA), and d18 (derived from palmitoyl-CoA) sphingolipids were quantified. Strikingly, d16 sphingolipids formed a major constituent of myocardial simple sphingolipids (Fig. 2 and supplemental Fig. 1), with approximately one-third of total DHS occurring with a 16-carbon alkyl chain in the sphingoid base (Fig. 2). In comparison, palmitate-derived d18:0-DHS accounted for slightly less than a third of DHS, and stearate-derived d20:0-DHS made up the remainder (data not shown). Similarly, one-third of the total dihydroceramide (DHC) pool contained a d16:0 base, whereas d18:0-DHC accounted for the other two-thirds of total DHC (Fig. 2). Curiously, no d20:0-DHC or ceramide was detected, suggesting that this species may serve as a poor substrate for CerS, which catalyzes *M*-acylation of sphingoid bases to generate DHC or ceramide (14). Surprisingly, despite the abundance of d16:0-DHC, d16:1-ceramide (d16:1-Cer) accounted for <2% of the total Cer pool (data not shown), and d16:1-sphingosine formed only about 6% of the total sphingosine pool (Fig. 2). This finding is consistent with previous data suggesting that dihydroceramide desaturase 1 (Des1), the enzyme that catalyzes the desaturation of DHC to Cer, utilizes DHC containing shorter chain sphingoid bases with less efficiency than d18:0-DHC (21). No d16 glycosphingolipids were detected, suggesting that further metabolism of d16:1-Cer may be limited (data not shown). Together, these findings indicate that myristate-derived sphingolipids form a part of the total cardiac simple sphingolipid pool. Furthermore, these data demonstrate that d16 sphingolipids are concentrated in the early metabolites of the sphingolipid synthetic pathway and suggest that they are utilized with alternative efficiencies by the sphingolipid biosynthetic enzymes downstream from CerS.

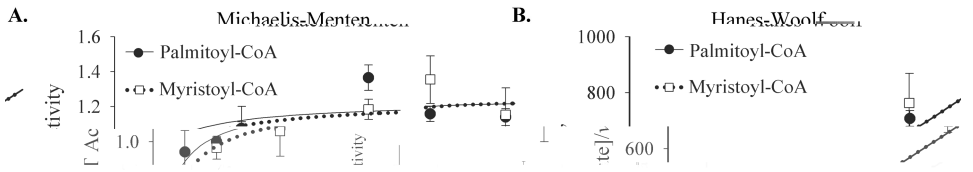

FIGURE 3. **Myocardial SPT utilizes myristoyl-CoA and palmitoyl-CoA similarly.** *A*, reaction velocities were similar between palmitoyl-CoA and myristoyl-CoA across substrate concentrations of 1.56–800 μM fatty acyl-CoA. Activities with concentrations of 1.56–100 μM fatty acyl-CoA are shown in detail in the *inset* (logarithmic scale). *B*, the Hanes-Woolf representation of these data revealed an inverse linear correlation between reaction velocity (*v*) and substrate concentration. Microsomal SPT was isolated from whole hearts of 12-week-old male C57Bl/6J mice and assayed with palmitoyl-CoA or myristoyl-CoA, as described under "Materials and Methods." Microsomes were generated from pooled homogenate from nine mice per assay. The assay was performed three times, with a total of 4–10 replicates/point. To allow robust comparisons between assays, data are presented as relative SPT activity, as described under "Materials and Methods." There were no statistically significant differences between palmitoyl-CoA and myristoyl-CoA utilization for the points tested ($p < 0.05$). Data are presented as mean ± S.E. (*error bars*).

TABLE 1

Kinetic analysis of SPT activity toward myristoyl-CoA and palmitoyl-CoA

Kinetic parameters, such as K_m, V_{max}, and the V_{max}/K_m ratio, are similar for myristoyl-CoA and palmitoyl-CoA utilization by endogenous cardiac SPT. Microsomal SPT was isolated from whole hearts and assayed, as described under "Materials and Methods." K_m was calculated using standardized data from all assays; V_{max} data are provided in units of relative activity, as described under "Materials and Methods." V_{max}/K_m is a relative measure of enzyme specificity for a particular substrate. Data are presented as means ± S.E.

	K_m	95% confidence interval	V_{max}	95% confidence interval	V_{max}/K_m
	μM				
Myristoyl-CoA	13.51 ± 2.20	9.11–17.90	1.24 ± 0.04	1.15–1.33	0.0917
Palmitoyl-CoA	9.72 ± 1.35	7.02–12.42	1.23 ± 0.35	1.16–1.30	0.1266

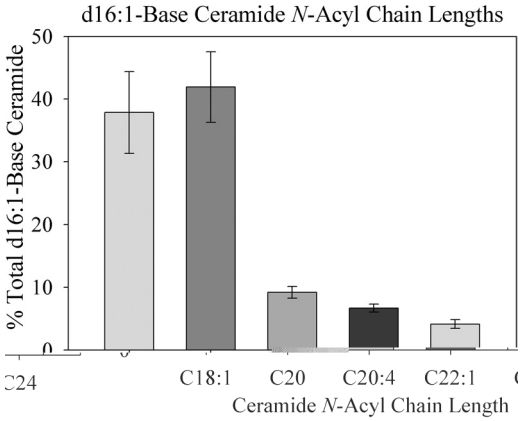

FIGURE 4. ***N*-Acyl chain length profile of myocardial d16:1-base ceramide.** Most d16:1 sphingoid bases partition into only a few *N*-acyl chain lengths of ceramide, particularly d16:1/$C_{18:1}$- and d16:1/$C_{20:0}$-ceramide. Hearts were harvested from six 16-week-old male C57Bl/6J mice, and lipids were extracted, analyzed by LC-MS, and normalized to protein as described under "Materials and Methods." Results are presented as mean ± S.E. (*error bars*).

such as $C_{16:0}$, that constitute major species of d18:1-Cer. Also striking is the relative abundance of the $C_{20:4}$ *M*-acyl chain, which is a minor species in d18:1-Cer (26, 27). Because each CerS isoform produces a unique pattern of *M*-acyl chain lengths (13, 28), these data suggested that specific CerS isoforms may catalyze the *M*-acylation of d16:0-DHS. This finding is particularly interesting in light of several recent studies on Cer *M*-acylation, which have identified specific signaling roles attributable to Cer of particular *M*-acyl chain lengths and CerS isoforms (29, 30).

In order to determine which CerS are responsible for *M*-acylation of d16 sphingoid bases, CerS activity was assayed [illegible]. Each CerS isoform was individually expressed and assayed with d16:0- or d18:0-DHS and several ^{14}C-labeled acyl-CoA substrates; results are shown for the acyl-CoA providing maximal activity for each CerS isoform (Fig. 5). All CerS isoforms used d16:0-DHS to some degree, displaying the same specificity toward the substrate for *M*-acylation as with d18:0-DHS (Fig. 5) (data not shown). Strikingly, only CerS1 displayed higher activity toward d16:0-DHS than toward d18:0-DHS (Fig. 5). In contrast, CerS2, CerS4, CerS5, and CerS6 all utilized d18:0-DHS more readily than d16:0-DHS (Fig. 5, and) (data not shown). Because CerS1 is expressed at low levels in the heart, it is likely that d16:0-DHS in the heart is *M*-acylated by other CerS isoforms (28). The preference for very long-chain fatty acyl-CoAs but not long-chain fatty acyl-CoAs, such as palmitoyl-CoA, suggests the involvement of CerS4 and possibly CerS2, both of which are robustly expressed in the myocardium (28, 31). Together, these results demonstrate that myristate- and palmitate-derived DHS are differentially utilized by individual CerS isoforms, suggesting that d16 sphingoid bases are further metabolized through uniquely defined metabolic routes.

[illegible] —Obesity and lipid overload have been shown to promote bioactive lipid production in the myocardium, partially due to oversupply of free fatty acids from the plasma, resulting in pathological cardiac remodeling and dysfunction (32, 33). Indeed, d18 sphingolipid chain length profiles were remodeled in a diet-

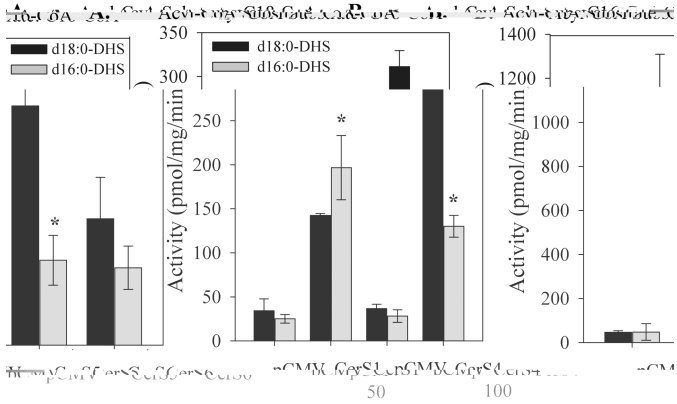

FIGURE 5. **CerS isoforms differentially utilize d16:0-dihydrosphingosine for dihydroceramide synthesis.** Cell extracts were prepared from cells overexpressing individual CerS or empty vector. CerS activity was assayed with d16:0- or d18:0-DHS and either [^{14}C]stearoyl-CoA (*A*) or [^{14}C]palmitoyl-CoA (*B*). Controls for CerS1, CerS5, and CerS6 were transfected with 50 μg of the

specific manner (20). However, it remains unknown whether d16 sphingolipids respond similarly to fatty acid overload.

In order to determine whether d16 simple sphingolipids increased in obesity, wild-type adult male C57Bl/6J mice were fed either a control diet or an obesogenic, diabetogenic high fat diet based on milk fat. This diet was highly enriched in saturated fat, particularly myristate, and promoted commensurate elevations in plasma free fatty acid profiles (20).[4] Lipidomic analysis revealed that the milk fat-based diet increased steady-state levels of total d16 simple sphingolipids (.d. DHS, sphingosine, DHC, Cer, DHS 1-phosphate, and sphingosine 1-phosphate) (Fig. 6) and d16:1-Cer (Fig. 6) in total heart extract. Furthermore, d16:1-Cer underwent chain length redistribution, with the proportion of d16:1-Cer containing a C18:1 *M*-acyl chain increasing markedly (Fig. 7) (data not shown). Notably, the increase in the levels and proportion of d16:1,C18:1-Cer, as opposed to unaltered or decreased levels of other species, may support the notion that CerS4 is the major CerS isoform responsible for d16:1-Cer production. This idea is further corroborated by the selective increase in CerS4, but not CerS2, expression upon feeding with the milk fat-based diet (Fig. 7). In contrast to these changes in d16:1-Cer levels and consistent with previous reports, levels of total d18 sphingolipids and total d18:1-Cer underwent essentially insignificant increases upon high fat feeding (Fig. 6). Levels of d20 sphingoid bases also did not change on the high fat diet, and no d20:0-DHC or d20:1-Cer was detected. In summary, these findings indicate that consumption of a diet rich in saturated fat is sufficient to stimulate accumulation of d16 sphingolipids $\mu\mu$.

To differentiate the effects of general fatty acid overload from the specific effects of a diet high in saturated fat, mice were fed either the milk fat-based diet described above or a traditional lard-based diet. In contrast to the milk fat-based diet, the lard-based diet was primarily enriched in unsaturated and polyunsaturated fatty acids and contained only approximately one-fourth of the myristate of the milk fat-based diet.[4] Animals were maintained on these diets for 18 weeks, and levels of d16:1-Cer and d16:0-DHC in the left ventricle were measured. This tissue was specifically studied because lipid overload has been linked to left ventricular hypertrophy and dysfunction (32–34), which comprise key features of diabetic cardiomyopathy in humans (35) and which we previously demonstrated in mice fed the milk fat-based high fat diet (20).

These analyses revealed that induction of d16:0-DHC and d16:1-Cer production by the milk fat diet was even more pronounced in the left ventricle than in whole heart lysate (Fig. 8). Furthermore, this accumulation was attenuated by treatment with the SPT inhibitor myriocin, indicating that these lipids derive from μ sphingolipid synthesis. In contrast, the lard diet did not promote significant production of d16 sphingolipids in the left ventricle. These findings suggest that dietary fat profiles, rather than total fatty acid content, serve as determinants of sphingolipid profiles in the left ventricle.

—Based on these findings, it appeared that dietary fatty acid oversupply could regulate d16 sphingolipid production in at least two ways. First, exposure to exogenous myristate might promote μ sphingolipid synthesis via increased substrate supply. This notion is supported by the observation that a diet high in myristate was sufficient to increase d16 sphingolipids (Fig. 8). Second, exposure to saturated fatty acids, which are generally elevated in the milk fat-based diet, could also increase SPTLC3 expression. This mode of regulation could be significant because the basal level of SPTLC3 expression has been shown to correlate directly with d16:0-DHS production in cancer cell lines (7).

To test whether increased d16 sphingolipid levels occurred specifically in response to myristate oversupply rather than as a general response to saturated fatty acid oversupply, isolated adult cardiomyocytes were cultured in the presence of myristate (C14:0) or palmitate (C16:0). Sphingolipids were extracted and measured by LC-MS. As observed in the intact myocardium, cultured cardiomyocytes harbored a significant amount of d16 sphingolipids basally, and exposure to myristate increased d16:1-Cer and d16:0-DHC (Fig. 9). In contrast, treatment with palmitate failed to increase levels of these metabolites. This suggests that oversupply of myristoyl-CoA, specifically, contributes to the production of cardiac d16 sphingolipids on a diet high in saturated fatty acids.

To test the second potential mechanism by which saturated fatty acids might up-regulate d16 sphingolipids, SPTLC3 expression was measured in isolated adult cardiomyocytes treated with myristate or palmitate, as above. Exposure to exogenous myristate increased SPTLC3 expression, as measured by qRT-PCR, whereas exposure to palmitate had no effect (Fig. 9). Together with the findings above, this indicates a specific role for myristate in regulation of d16 sphingolipid production, possibly through a combination of substrate supply and direct regulation of SPTLC3 expression. Moreover, these data underscore the finding that dietary fat composition regulates cardiac sphingolipid profiles.

[4] T. Geng, W. Hu, M. H. Broadwater, J. Snider, J. Bielawski, S. B. Russo, J. Schwacke, J. S. Ross, L. A. Cowart, manuscript in preparation.

—Although this and previous reports have elucidated aspects of SPTLC3 expression and enzymology, it remains unknown whether d16 sphingolipids are functionally equivalent to canonical d18 sphingolipids. We recently demonstrated that myristate treatment promoted autophagic flux in cardiomyocytes in a sphingolipid-dependent manner, probably by promoting synthesis of d18:1/C_{14}-Cer, in which myristate is incorporated as the *M*-acyl, rather than alkyl, chain (20). Because myristate treatment also stimulated production of d16:0-DHS and its derivatives (Fig. 9) (data not shown), this led us to ask whether sphingolipids bearing myristate-derived alkyl chains might also contribute to the proautophagic effect of myristate. This question is of particular importance, because myristate-induced autophagy has been implicated in cardiomyocyte hypertrophy in lipid overload (20).

Two approaches were used to determine whether SPTLC3 and d16:0-DHS mediate myristate-induced autophagy. In the first, isolated adult primary cardiomyocytes were treated with either d18:0-DHS or d16:0-DHS, and expression of the autophagy markers Beclin 1 and Atg7 was measured by qRT-PCR. Consistent with previous results (20), treatment with d18:

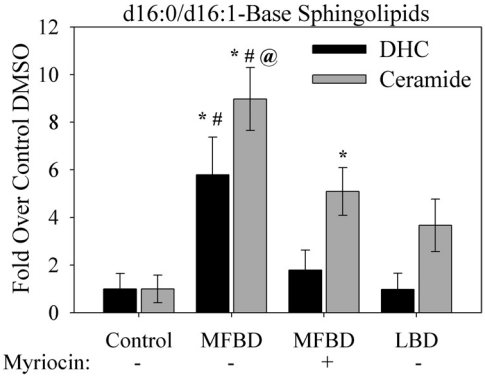

FIGURE 8. **A diet high in myristate stimulates d16 sphingolipid production in the left ventricle.** Feeding with a milk fat-based high fat diet (*MFBD*) (60% kcal from fat), which is high in myristate and total saturated fat, increased total levels of d16:0-DHC and d16:1-ceramide. This was inhibited by treatment with myriocin. In contrast, feeding with a lard-based high fat diet (*LBD*

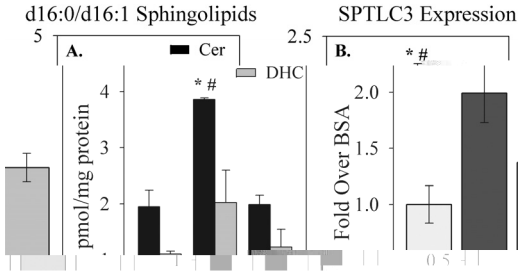

FIGURE 9. **Control of d16 sphingolipid levels and SPTLC3 expression by fatty acids.** *A*, treatment with the saturated fatty acid myristate (*Myr*; C14:0), but not palmitate (*Pal*; C16:0), stimulated production of d16:1-ceramide (*Cer*) and d16:0-dihydroceramide (*DHC*). *B*, myristate, but not palmitate, treatment also stimulated an increase in SPTLC3 mRNA levels. Primary adult cardiomyocytes were treated with BSA or fatty acid conjugated to BSA, as indicated, for 16 h. Lipids and RNA were extracted and prepared for analysis by LC-MS or qRT-PCR, respectively, as indicated under "Materials and Methods." Results are presented as mean ± S.E. (*error bars*). *, $p < 0.05$ *versus* BSA; #, $p < 0.05$ *versus* palmitate.

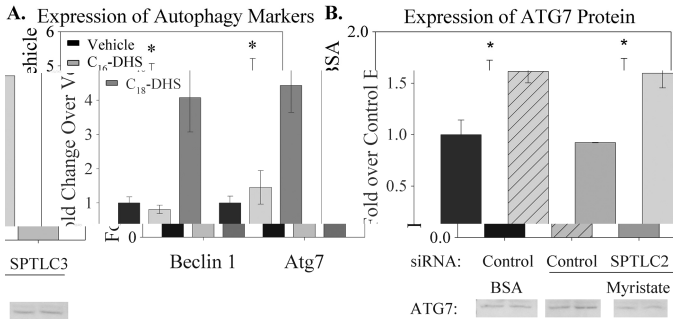

FIGURE 10. **SPTLC3 and d16:0-DHS did not contribute to myristate-induced sphingolipid-dependent autophagy.** *A*, treatment with d18:0-DHS induced expression of the autophagy markers Beclin 1 and Atg7. In contrast, treatment with d16:0-DHS did not induce Beclin 1 or Atg7 expression. Primary adult cardiomyocytes were treated with vehicle or with 2.5 μM d18:0-DHS or d16:0-DHS, as indicated, for 3 h. RNA was extracted and analyzed by qRT-PCR as indicated under "Materials and Methods." *B*, knockdown of SPTLC2, but not SPTLC3, protected isolated cardiomyocytes from overexpression of the autophagy marker Atg7. Cells were transfected with siRNA for 24 h and then treated with BSA or 0.l mM myristate for 16 h, as described under "Materials and Methods." Quantifications of immunoblots are presented with representative images; non-contiguous *lanes*, separated by *white lines*, are shown from the same gel. All results are presented as mean ± S.E. (*error bars*). *, $p <$ 0.05 *versus* vehicle or BSA plus control siRNA.

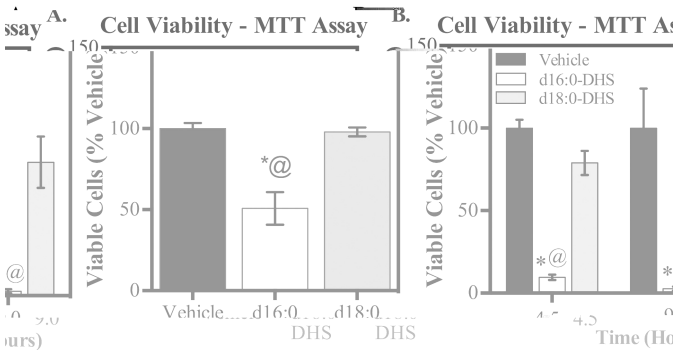

FIGURE 11. **d16:0-DHS treatment diminished cell viability in cardiomyocytes.** Treatment with 2.5 μM d16:0-DHS, but not d18:0-DHS, diminished cell viability of H9c2 immortalized cardiomyocytes, as determined by the MTT assay. *A*, cells were treated for 3 h and subjected to the MTT assay, as described under "Materials and Methods." *B*, even over an extended time course of 4.5 and 9 h, cell viability was reduced selectively by d16:0-DHS but not d18:0-DHS. There was no significant difference between vehicle groups at 4.5 and 9 h of sphingoid base treatment ($p = 0.6$). Results are presented as a percentage of vehicle for each time point and given as mean ± S.E. (*error bars*). *, $p < 0.05$ *versus* vehicle; @, $p < 0.05$ *versus* d18:0-DHS.

0-DHS stimulated expression of autophagy markers, compared with vehicle (Fig. 10). In contrast, d16:0-DHS treatment did not result in overexpression of either Beclin 1 or Atg7. Suggesting that this lack of effect is not merely due to insufficient or excessive d16:0-DHS concentration, treatment of H9c2 immortalized cardiomyocytes with a range of 0.625–5 μM d16:0-DHS did not induce expression of autophagy markers (data not shown). This suggests that d18:0-DHS and d16:0-DHS may play distinct roles in this cellular process.

However, to test definitively whether SPTLC3 and its d16:0 products were functionally disparate from SPTLC2, cells were subjected to siRNA-mediated knockdown of either SPTLC2 or SPTLC3, and expression of autophagy markers was measured by Western blot after treatment with myristate. Consistent with the known role of d18:0 sphingolipids in autophagy, knockdown of SPTLC2 prevented induction of Atg7 protein expression (Fig. 10). In contrast, knockdown of SPTLC3 failed to prevent an increase in Atg7 protein in response to myristate. Similarly, myristate-induced autophagic flux, as indicated by lipidation and degradation of the autophagy protein LC3B, was prevented by knockdown of SPTLC2 but not SPTLC3 (data not shown). These results suggest that SPTLC2, but not SPTLC3, is required for myristate-dependent induction of autophagy in cardiomyocytes.

d ax 16 f —In addition to autophagy, cell death is a major sphingolipid-associated cellular outcome (36). However, all previous data addressed d18 sphingolipids specifically or utilized methods (such as pharmacologic inhibitors of SPT or CerS) that do not distinguish among species based on alkyl chain length. Due to the differential effects of d16 and d18 sphingolipids on induction of autophagy, we examined whether cell death might also occur in an alkyl chain length-dependent manner in cardiomyocytes.

To test this, H9c2 immortalized cardiomyocytes were treated with d16:0- or d18:0-DHS, and cell viability was assessed by an MTT assay. Strikingly, whereas treatment with d18:0-DHS had no effect, treatment with d16:0-DHS significantly promoted cell death (Fig. 11). This difference held true over an extended time course (Fig. 11). Suggesting that this cell death might be mediated, at least in part, through apoptosis, treatment of primary adult cardiomyocytes with d16:0-DHS, but not d18:0-DHS, promoted cleavage of the nuclear enzyme PARP, which is an important marker of apoptosis (Fig. 12) (37). These findings, together with the observations of differential effects of d16 and d18 sphingolipids on autophagy, provide the first direct evidence that d16 and d18 sphingolipids have non-overlapping molecular roles in the heart.

DISCUSSION

The regulation of sphingolipid production in the heart is a subject of considerable interest, especially in light of the known involvement of sphingolipids in multiple forms of cardiac pathology (reviewed in Ref. 38). However, most studies have examined the effects of modulating bulk sphingolipid produc-

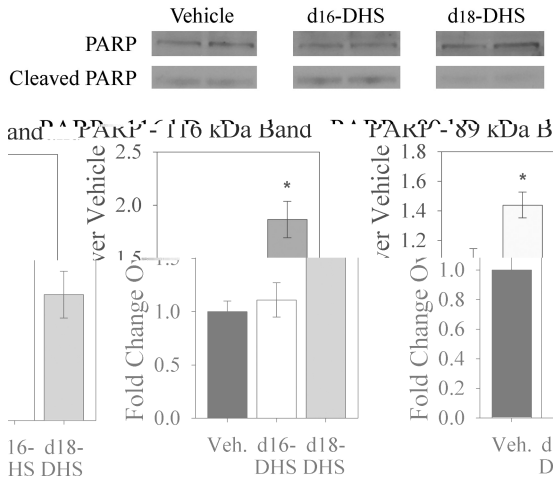

FIGURE 12. **d16:0-DHS treatment promoted PARP cleavage in cardiomyocytes.** Treatment with d18:0-DHS resulted in increased expression of the intact PARP enzyme (116 kDa) but did not increase levels of its cleaved form (89 kDa). In contrast, d16:0-DHS treatment increased levels of the cleaved form of PARP but not of its intact form. Primary adult cardiomyocytes were treated with vehicle or with 2.5 μM d18:0-DHS or d16:0-DHS, as indicated, for 3 h. Cells were subject to immunoblotting, as described under "Materials and Methods." Quantifications are shown with images from a representative immunoblot. *Top* and *bottom bands* of PARP are shown from different exposures of the same *lanes* in order to prevent image oversaturation. In our hands under the present culture conditions, primary cardiomyocytes displayed a low but detectable basal level of PARP cleavage and cell death; however, this is normal for this cell type under these conditions. Quantifications of immunoblots were normalized to actin and are presented as mean ± S.E. (*error bars*). *, $p < 0.05$ *versus* vehicle.

tion, with roles for individual sphingolipid species and the metabolic routes from which they derive remaining largely undefined. Thus, identification of mechanisms by which cardiac sphingolipid profiles are regulated, particularly under pathological conditions, such as lipid overload, may reveal novel therapeutic targets.

The present study defines the production and metabolism of non-canonical myristate-derived sphingolipids in the myocardium. Although previous studies revealed that myristate-derived d16:0-DHS is produced by the SPTLC3 subunit of SPT (7), no information is available about the subsequent metabolism of this sphingoid base or about the regulation of the SPTLC3 subunit. The present study demonstrated that microsomal SPT derived from myocardium, which robustly expresses SPTLC3, readily utilized myristoyl-CoA [illegible]. Indeed, SPT utilized myristoyl-CoA and palmitoyl-CoA equally well, mirroring the relative levels of d16:0- and d18:0-DHS observed [illegible]. These sphingolipid profiles also accord well with basal [illegible] acyl-CoA levels; myristoyl-CoA and palmitoyl-CoA are equally abundant in the myocardium (39). In addition to d16 and d18 sphingolipids, some d20:0-DHS and d20:1-sphingosine were also detected in the heart. However, no d20:0-DHC or d20:1-Cer were found to be present. Because sphingosine is produced by deacylation of Cer, this suggests that these bases may be taken up from the plasma. Furthermore, a very recent report suggests that d20 sphingoid bases may be produced through SPTLC2, in combination with a putative small subunit of SPT (40).

This study also provided the first account of the metabolism of d16:0-DHS, bringing to light a potential for improvement in current lipidomic strategies. Standard LC-MS-based detection methods may overlook species not specifically targeted for analysis (41). Because it was heretofore unknown that d16 sphingolipids constituted an appreciable proportion of simple sphingolipids in some tissues, analyses have been selectively focused on detection of traditional d18 sphingolipids. However, based on data presented here, we propose that analyses of tissues highly expressing SPTLC3 might be more comprehensive if d16 sphingolipid levels were also taken into account. This bears particular relevance to experimental contexts in which no increase in d18 sphingolipids was detected, yet inhibition of SPT by myriocin was found to be protective.

Because subunit expression profiles may differ across species and are sensitive to dietary fat composition and possibly other variables, it may be beneficial to measure SPTLC3 expression or basal d16 sphingolipid levels when designing and interpreting sphingolipid-oriented studies. For example, in our hands, SPTLC3 was not richly expressed in the livers of 12-week-old male mice maintained on standard laboratory chow (data not shown), whereas a previous report indicated that SPTLC3 is abundantly expressed in human liver (19). Thus, there may be roles for SPTLC3 in the human liver that would have been missed by investigations in those mice. Likewise, disparities were observed between circulating sphingoid base levels in mice and humans. Whereas circulating levels of d18 sphingoid bases were similar, the concentration of d16 sphingoid bases in murine plasma was only about 10% of that observed in humans (7). This could possibly result in significant functional differences; d16 sphingoid bases comprise as much as 15% of total circulating sphingoid bases in humans and have been suggested as a potential biomarker for type 2 diabetes (7, 42). Because circulating sphingolipids have been shown to act on tissues other than their tissue of origin (43), circulating d16 sphingolipids may affect tissues that do not produce them endogenously, if they are present in sufficient amounts. In contrast to these two examples, this study found that expression of SPT subunits in the murine heart reflected those previously reported in humans, supporting the potential relevance of results in this system to human health (19). Furthermore, SPTLC3 expression was shown to be responsive to exogenous myristate levels through an unknown mechanism, possibly involving myristoylation of transcription factors or regulatory proteins. These findings illustrate the need to be aware of variations in SPTLC3 expression and d16 SL levels across model systems, especially when assessing the clinical relevance of experimental outcomes.

In the present study, LC-MS analyses revealed that myocardial d16 sphingolipids form similar proportions of DHS and DHC but are not further metabolized efficiently, comprising only a very small amount of total Cer and sphingosine. This suggests that d16:0-DHS may be poorly utilized by the dihydroceramide desaturase enzyme Des1, which converts DHC to Cer (44); alternatively, it may be sequestered from Des1 through differential targeting to cell membranes or organelles. Because numerous studies indicate distinct roles for DHC and Cer, the lack of conversion of d16:0-DHC to d16:1-Cer may represent sequestration of these lipids from further metabolism that could promote pathological processes. On the other hand, our

data do not preclude other explanations, such as addition of specific headgroups to d16:0-DHC, rapid metabolism of d16:1-Cer to sphingomyelin, or differential rates of turnover of d16 sphingolipids. Notably, d16:1-Cer was much more abundant in isolated feline cardiomyocytes, compared with total myocardial extract from mice. This may be due to confounding nonmyocytes, such as fibroblasts, in the total myocardial lysate; to interspecies differences in Des1p substrate preferences; or to metabolic differences between working and quiescent cardiomyocytes.

Intriguingly, data showed that d16:0-DHS was only metabolized to d16:0-DHC and d16:1-Cer containing selected *M*-acyl chains, predominantly C18:1 and C20:0. These results prompted investigations into the [illegible] utilization of d16:0-DHS by individual CerS isoforms, which revealed CerS1 to be the only CerS enzyme that preferentially utilized d16:0-DHS, compared with the canonical d18:0-DHS. Despite this, it appears more likely that other CerS isoforms, specifically CerS4 and possibly CerS2, mediate *M*-acylation of d16:0-DHS in the heart. This notion is based on known patterns of CerS expression in the heart and the observed *M*-acyl profiles in this study. Specifically, the heart primarily expresses CerS2, CerS4, and CerS5, with very little CerS1 being detected (28, 31). Furthermore, the bias of d16:1-Cer and d16:0-DHC *M*-acyl profiles toward very long-chain fatty acids suggests that CerS5, which produces only long-chain Cer, is a less important player than CerS2 and CerS4 (28, 31). Because CerS4 is the most highly expressed CerS isoform in the heart (45), produces the major *M*-acyl chain lengths observed in d16 DHC and Cer, and was up-regulated under conditions that promoted d16 DHC and Cer production, it appears that CerS4 may be the major isoform of d16 DHC and Cer synthesis in the heart. Future experiments will test this hypothesis and its functional implications directly. In addition to these findings, it should be noted that, although CerS activity comprises the canonical route of DHC and Cer synthesis, some stress conditions may activate reverse ceramidase activity, which synthesizes Cer from sphingosine and an acyl-CoA; this pathway is most prominent in the mitochondria (27, 46). Although reverse ceramidase activity does not account for a major proportion of basal d18:1-Cer synthesis, its impact on d16:1-Cer metabolism remains to be assessed.

Increases in bulk sphingolipids have been shown to lead to cardiac hypertrophy and dysfunction in lipid overload (32, 47). Although [illegible] sphingolipid synthesis has been implicated in many pathological aspects of heart disease (reviewed in Ref. 38), only limited information is available about the roles of specific sphingolipids in these processes (20). Recent studies have indicated that plasma lipid profiles in obese individuals demonstrate a shift toward shorter, saturated acyl chains, such as myristate, which can be utilized by SPTLC3 for sphingoid base synthesis (7, 48). Furthermore, we recently reported that feeding with a high fat diet rich in myristate promoted sphingolipid-dependent cardiac dysfunction and hypertrophy (20). These findings were recapitulated in isolated cardiomyocytes; myristate oversupply, but not oversupply of palmitate, induced pathological sphingolipid-dependent autophagy and subsequent autophagy-dependent hypertrophy. Because the present study has demonstrated that oversupply of myristate, but not palmitate, selectively potentiated SPTLC3 expression and d16:1-Cer and d16:0-DHC production, we examined whether d16 sphingolipids might contribute to the proautophagic effect of myristate. Surprisingly, whereas d18:0-DHS treatment promoted overexpression of Beclin 1 and Atg7, treatment with d16:0-DHS had no such effect. Indicating that this was not merely a dose- or time-dependent difference between exogenous base treatments, knockdown of SPTLC2, but not SPTLC3, was sufficient to prevent induction of Atg7 expression and autophagic flux by myristate, demonstrating the first known difference in biochemical roles between SPTLC2 and SPTLC3.

These results indicated distinct functions for SPTLC2 and SPTLC3 as well as their products. This notion was further supported by evidence from a heart-specific SPTLC2 knock-out mouse (49). In this model, loss of SPTLC2 led to cardiac dysfunction, hypertrophy, and fibrosis. Although SPTLC3 expression increased spontaneously upon SPTLC2 ablation, it was insufficient to prevent these deleterious outcomes. The present study indicated that treatment with d16:0-DHS, but not d18:0-DHS, dramatically induced cell death in H9c2 immortalized cardiomyocytes. Furthermore, only d16:0-DHS treatment promoted PARP cleavage, which is a key proapoptotic event (37), in isolated a248(no155ldf5.3(PARP)-a.9(a(b1(In)-2aos)-2-209.8lectively534

bined (20) (data not shown). Although d16 sphingolipids appear to be proapoptotic, autophagic cell death may be more prevalent in the failing heart, and antiapoptotic programs may be sufficient to antagonize the proapoptotic effects of d16 sphingolipids (52, 53). We thereby speculate that production of d16:0-DHS, which did not induce autophagy, may act as a metabolic sink for myristoyl-CoA that could otherwise be utilized for production of cardiotoxic lipids.

Another possible role for d16 sphingolipids stems from their biophysical effects; *M*-acyl chain lengths of sphingolipid species have been shown to impact numerous important membrane properties, which in turn modulate activity of some membrane-resident proteins (18, 54–63). Likewise, incorporation of short-chain sphingolipids into cellular membranes could alter membrane curvature and fluidity, producing downstream effects in a manner independent of traditional signaling modalities. Future studies will aim to test these hypotheses and to identify potential signaling roles of d16 sphingolipids in the myocardium.

In conclusion, SPTLC3 is highly expressed in the myocardium and in isolated cardiomyocytes. Increased incorporation of the SPTLC3 subunit alters acyl-CoA selectivity of the SPT complex, and its products are differentially utilized by the enzymes of sphingolipid metabolism. Moreover, concentrations of these metabolites respond positively to exogenous myristate levels and high myristate feeding, possibly as a protective regulatory feedback loop. Indeed, SPTLC3 could potentially function as a regulatory switch that routes myristoyl-CoA into DHS, thereby preventing its incorporation into d18:1/$C_{14:0}$-Cer, a metabolite with cardiotoxic properties. Additionally, signaling functions of d16:0-DHS and d18:0-DHS appear to be distinct, possibly due to differential metabolism into downstream bioactive sphingolipids. Specific roles for d16:0-DHS and its derivatives in the heart and their potential involvement in the regulation of cell death remain under investigation. These hypotheses will be tested in ongoing studies, which seek to address the specific functions of SPTLC3 and d16 sphingolipids in the myocardium as well as to test the potential role of SPTLC3 as a metabolic routing switch.

REFERENCES

1. Cowart, L. A. (2009) Sphingolipids. Players in the pathology of metabolic disease. *Trends Endocrinol. Metab.* **20,** 34–42
2. Bartke, N., and Hannun, Y. A. (2009) Bioactive sphingolipids. Metabolism and function. *J. Lipid Res.* **50**, S91–S96
3. Brice, S. E., and Cowart, L. A. (2011) Sphingolipid metabolism and analysis in metabolic disease. *Adv. Exp. Med. Biol.* **721,** 1–17
4. Hanada, K. (2003) Serine palmitoyltransferase, a key enzyme of sphingolipid metabolism. *Biochim. Biophys. Acta* **1632,** 16–30
5. Gault, C. R., Obeid, L. M., and Hannun, Y. A. (2010) An overview of sphingolipid metabolism. From synthesis to breakdown. *Adv. Exp. Med. Biol.* **688,** 1–23
6. Hornemann, T., Wei, Y., and von Eckardstein, A. (2007) Is the mammalian serine palmitoyltransferase a high-molecular-mass complex? *Biochem. J.* **405,** 157–164
7. Hornemann, T., Penno, A., Rütti, M. F., Ernst, D., Kivrak-Pfiffner, F., Rohrer, L., and von Eckardstein, A. (2009) The SPTLC3 subunit of serine palmitoyltransferase generates short chain sphingoid bases. *J. Biol. Chem.* **284,** 26322–26330
8. Han, G., Gupta, S. D., Gable, K., Niranjanakumari, S., Moitra, P., Eichler, F., Brown, R. H., Jr., Harmon, J. M., and Dunn, T. M. (2009) Identification of small subunits of mammalian serine palmitoyltransferase that confer distinct acyl-CoA substrate specificities. *Proc. Natl. Acad. Sci. U.S.A.* **106,** 8186–8191
9. Jenkins, G. M., Cowart, L. A., Signorelli, P., Pettus, B. J., Chalfant, C. E., and Hannun, Y. A. (2002) Acute activation of *de novo* sphingolipid biosynthesis upon heat shock causes an accumulation of ceramide and subsequent dephosphorylation of SR proteins. *J. Biol. Chem.* **277,** 42572–42578
10. Kent, R. L., Mann, D. L., Urabe, Y., Hisano, R., Hewett, K. W., Loughnane, M., and Cooper, G., 4th (1989) Contractile function of isolated feline cardiocytes in response to viscous loading. *Am. J. Physiol.* **257,** H1717–H1727
11. Hu, W., Bielawski, J., Samad, F., Merrill, A. H., Jr., and Cowart, L. A. (2009) Palmitate increases sphingosine-1-phosphate in C2C12 myotubes via up-regulation of sphingosine kinase message and activity. *J. Lipid Res.* **50,** 1852–1862
12. Bielawski, J., Szulc, Z. M., Hannun, Y. A., and Bielawska, A. (2006) Simultaneous quantitative analysis of bioactive sphingolipids by high-performance liquid chromatography-tandem mass spectrometry. *Methods* **39,** 82–91
13. Tidhar, R., Ben-Dor, S., Wang, E., Kelly, S., Merrill, A. H., Jr., and Futerman, A. H. (2012) Acyl chain specificity of ceramide synthases is determined within a region of 150 residues in the Tram-Lag-CLN8 (TLC) domain. *J. Biol. Chem.* **287,** 3197–3206
14. Pewzner-Jung, Y., Ben-Dor, S., and Futerman, A. H. (2006) When do Lasses (longevity assurance genes) become CerS (ceramide synthases)? Insights into the regulation of ceramide synthesis. *J. Biol. Chem.* **281,** 25001–25005
15. Futerman, A. H., and Hannun, Y. A. (2004) The complex life of simple sphingolipids. *EMBO Rep.* **5,** 777–782
16. Rotstein, N. P., Miranda, G. E., Abrahan, C. E., and German, O. L. (2010) Regulating survival and development in the retina. Key roles for simple sphingolipids. *J. Lipid Res.* **51,** 1247–1262
17. Goñi, F. M., and Alonso, A. (2006) Biophysics of sphingolipids I. Membrane properties of sphingosine, ceramides and other simple sphingolipids. *Biochim. Biophys. Acta* **1758,** 1902–1921
18. Goñi, F. M., and Alonso, A. (2009) Effects of ceramide and other simple sphingolipids on membrane lateral structure. *Biochim. Biophys. Acta* **1788,** 169–177
19. Hornemann, T., Richard, S., Rütti, M. F., Wei, Y., and von Eckardstein, A. (2006) Cloning and initial characterization of a new subunit for mammalian serine-palmitoyltransferase. *J. Biol. Chem.* **281,** 37275–37281
20. Russo, S. B., Baicu, C. F., Van Laer, A., Geng, T., Kasiganesan, H., Zile, M. R., and Cowart, L. A. (2012) Ceramide synthase 5 mediates lipid-induced autophagy and hypertrophy in cardiomyocytes. *J. Clin. Invest.* **122,** 3919–3930
21. Michel, C., van Echten-Deckert, G., Rother, J., Sandhoff, K., Wang, E., and Merrill, A. H., Jr. (1997) Characterization of ceramide synthesis. A dihydroceramide desaturase introduces the 4,5-*trans*-double bond of sphingosine at the level of dihydroceramide. *J. Biol. Chem.* **272,** 22432–22437
22. Williams, R. D., Sgoutas, D. S., and Zaatari, G. S. (1986) Enzymology of long-chain base synthesis by aorta. Induction of serine palmitoyltransferase activity in rabbit aorta during atherogenesis. *J. Lipid Res.* **27,** 763–770
23. Merrill, A. H., Jr., and Williams, R. D. (1984) Utilization of different fatty acyl-CoA thioesters by serine palmitoyltransferase from rat brain. *J. Lipid Res.* **25,** 185–188
24. Merrill, A. H., Jr., Nixon, D. W., and Williams, R. D. (1985) Activities of serine palmitoyltransferase (3-ketosphinganine synthase) in microsomes from different rat tissues. *J. Lipid Res.* **26,** 617–622

25. National Research Council (1985) *Guide for the Care and Use of Laboratory Animals*, National Institutes of Health Publication 85-23, National Institutes of Health, Bethesda, MD
26. Mullen, T. D., Spassieva, S., Jenkins, R. W., Kitatani, K., Bielawski, J., Hannun, Y. A., and Obeid, L. M. (2011) Selective knockdown of ceramide synthases reveals complex interregulation of sphingolipid metabolism. *J. Lipid Res.* **52,** 68–77
27. Novgorodov, S. A., Wu, B. X., Gudz, T. I., Bielawski, J., Ovchinnikova, T. V., Hannun, Y. A., and Obeid, L. M. (2011) Novel pathway of ceramide production in mitochondria. Thioesterase and neutral ceramidase produce ceramide from sphingosine and acyl-CoA. *J. Biol. Chem.* **286,** 25352–25362
28. Laviad, E. L., Albee, L., Pankova-Kholmyansky, I., Epstein, S., Park, H., Merrill, A. H., Jr., and Futerman, A. H. (2008) Characterization of ceramide synthase 2. Tissue distribution, substrate specificity, and inhibition by sphingosine 1-phosphate. *J. Biol. Chem.* **283,** 5677–5684
29. Senkal, C. E., Ponnusamy, S., Bielawski, J., Hannun, Y. A., and Ogretmen, B. (2010) Antiapoptotic roles of ceramide-synthase-6-generated C16-ceramide via selective regulation of the ATF6/CHOP arm of ER-stress-response pathways. *FASEB J.* **24,** 296–308
30. Senkal, C. E., Ponnusamy, S., Rossi, M. J., Bialewski, J., Sinha, D., Jiang, J. C., Jazwinski, S. M., Hannun, Y. A., and Ogretmen, B. (2007) Role of human longevity assurance gene 1 and C18-ceramide in chemotherapy-induced cell death in human head and neck squamous cell carcinomas. *Mol. Cancer Ther.* **6,** 712–722
31. Riebeling, C., Allegood, J. C., Wang, E., Merrill, A. H., Jr., and Futerman, A. H. (2003) Two mammalian longevity assurance gene (LAG1) family members, trh1 and trh4, regulate dihydroceramide synthesis using different fatty acyl-CoA donors. *J. Biol. Chem.* **278,** 43452–43459
32. Park, T. S., Hu, Y., Noh, H. L., Drosatos, K., Okajima, K., Buchanan, J., Tuinei, J., Homma, S., Jiang, X. C., Abel, E. D., and Goldberg, I. J. (2008) Ceramide is a cardiotoxin in lipotoxic cardiomyopathy. *J. Lipid Res.* **49,** 2101–2112
33. van de Weijer, T., Schrauwen-Hinderling, V. B., and Schrauwen, P. (2011) Lipotoxicity in type 2 diabetic cardiomyopathy. *Cardiovasc. Res.* **92,** 10–18
34. Bugger, H., and Abel, E. D. (2009) Rodent models of diabetic cardiomyopathy. *Dis. Model. Mech.* **2,** 454–466
35. Guha, A., Harmancey, R., and Taegtmeyer, H. (2008) Nonischemic heart failure in diabetes mellitus. *Curr. Opin. Cardiol.* **23,** 241–248
36. Mimeault, M. (2002) New advances on structural and biological functions of ceramide in apoptotic/necrotic cell death and cancer. *FEBS Lett.* **530,** 9–16
37. Wieder, T., Geilen, C. C., Kolter, T., Sadeghlar, F., Sandhoff, K., Brossmer, R., Ihrig, P., Perry, D., Orfanos, C. E., and Hannun, Y. A. (1997) Bcl-2 antagonizes apoptotic cell death induced by two new ceramide analogues. *FEBS Lett.* **411,** 260–264
38. Baranowski, M., and Górski, J. (2011) Heart sphingolipids in health and disease. *Adv. Exp. Med. Biol.* **721,** 41–56
39. Harmancey, R., Wilson, C. R., Wright, N. R., and Taegtmeyer, H. (2010) Western diet changes cardiac acyl-CoA composition in obese rats. A potential role for hepatic lipogenesis. *J. Lipid Res.* **51,** 1380–1393
40. Harmon, J. M., Bacikova, D., Gable, K., Gupta, S. D., Han, G., Sengupta, N., Somashekarappa, N., and Dunn, T. M. (February 20, 2013) Topological and functional characterization of the ssSPTs, small activating subunits of serine palmitoyltransferase. *J. Biol. Chem.* 10.1074/jbc.M113.451526
41. Sullards, M. C., Allegood, J. C., Kelly, S., Wang, E., Haynes, C. A., Park, H., Chen, Y., and Merrill, A. H., Jr. (2007) Structure-specific, quantitative methods for analysis of sphingolipids by liquid chromatography-tandem mass spectrometry. "Inside-out" sphingolipidomics. *Methods Enzymol.* **432,** 83–115
42. Othman, A., Rütti, M. F., Ernst, D., Saely, C. H., Rein, P., Drexel, H., Porretta-Serapiglia, C., Lauria, G., Bianchi, R., von Eckardstein, A., and Hornemann, T. (2012) Plasma deoxysphingolipids. A novel class of biomarkers for the metabolic syndrome? *Diabetologia* **55,** 421–431
43. Igarashi, J., and Michel, T. (2008) The enigma of sphingosine 1-phosphate synthesis. A novel role for endothelial sphingosine kinases. *Circ. Res.* **102,** 630–632
44. Ternes, P., Franke, S., Zähringer, U., Sperling, P., and Heinz, E. (2002) Identification and characterization of a sphingolipid δ 4-desaturase family. *J. Biol. Chem.* **277,** 25512–25518
45. Levy, M., and Futerman, A. H. (2010) Mammalian ceramide synthases. *IUBMB Life* **62,** 347–356
46. El Bawab, S., Birbes, H., Roddy, P., Szulc, Z. M., Bielawska, A., and Hannun, Y. A. (2001) Biochemical characterization of the reverse activity of rat brain ceramidase. A CoA-independent and fumonisin B1-insensitive ceramide synthase. *J. Biol. Chem.* **276,** 16758–16766
47. Dyntar, D., Eppenberger-Eberhardt, M., Maedler, K., Pruschy, M., Eppenberger, H. M., Spinas, G. A., and Donath, M. Y. (2001) Glucose and palmitic acid induce degeneration of myofibrils and modulate apoptosis in rat adult cardiomyocytes. *Diabetes* **50,** 2105–2113
48. Rhee, E. P., Cheng, S., Larson, M. G., Walford, G. A., Lewis, G. D., McCabe, E., Yang, E., Farrell, L., Fox, C. S., O'Donnell, C. J., Carr, S. A., Vasan, R. S., Florez, J. C., Clish, C. B., Wang, T. J., and Gerszten, R. E. (2011) Lipid profiling identifies a triacylglycerol signature of insulin resistance and improves diabetes prediction in humans. *J. Clin. Invest.* **121,** 1402–1411
49. Lee, S. Y., Kim, J. R., Hu, Y., Khan, R., Kim, S. J., Bharadwaj, K. G., Davidson, M. M., Choi, C. S., Shin, K. O., Lee, Y. M., Park, W. J., Park, I. S., Jiang, X. C., Goldberg, I. J., and Park, T. S. (2012) Cardiomyocyte specific deficiency of serine palmitoyltransferase subunit 2 reduces ceramide but leads to cardiac dysfunction. *J. Biol. Chem.* **287,** 18429–18439
50. Mirkov, S., Myers, J. L., Ramírez, J., and Liu, W. (2012) SNPs affecting serum metabolomic traits may regulate gene transcription and lipid accumulation in the liver. *Metabolism* **61,** 1523–1527
51. Hicks, A. A., Pramstaller, P. P., Johansson, A., Vitart, V., Rudan, I., Ugocsai, P., Aulchenko, Y., Franklin, C. S., Liebisch, G., Erdmann, J., Jonasson, I., Zorkoltseva, I. V., Pattaro, C., Hayward, C., Isaacs, A., Hengstenberg, C., Campbell, S., Gnewuch, C., Janssens, A. C., Kirichenko, A. V., König, I. R., Marroni, F., Polasek, O., Demirkan, A., Kolcic, I., Schwienbacher, C., Igl, W., Biloglav, Z., Witteman, J. C., Pichler, I., Zaboli, G., Axenovich, T. I., Peters, A., Schreiber, S., Wichmann, H. E., Schunkert, H., Hastie, N., Oostra, B. A., Wild, S. H., Meitinger, T., Gyllensten, U., van Duijn, C. M., Wilson, J. F., Wright, A., Schmitz, G., and Campbell, H. (2009) Genetic determinants of circulating sphingolipid concentrations in European populations. *PLoS Genet.* **5,** e1000672
52. Chiong, M., Wang, Z. V., Pedrozo, Z., Cao, D. J., Troncoso, R., Ibacache, M., Criollo, A., Nemchenko, A., Hill, J. A., and Lavandero, S. (2011) Cardiomyocyte death. Mechanisms and translational implications. *Cell Death Dis.* **2,** e244
53. Knaapen, M. W., Davies, M. J., De Bie, M., Haven, A. J., Martinet, W., and Kockx, M. M. (2001) Apoptotic versus autophagic cell death in heart failure. *Cardiovasc. Res.* **51,** 304–312
54. Dupuy, F., Fanani, M. L., and Maggio, B. (2011) Ceramide *N*-acyl chain length. A determinant of bidimensional transitions, condensed domain morphology, and interfacial thickness. *Langmuir* **27,** 3783–3791
55. Nybond, S., Björkqvist, Y. J., Ramstedt, B., and Slotte, J. P. (2005) Acyl chain length affects ceramide action on sterol/sphingomyelin-rich domains. *Biochim. Biophys. Acta* **1718,** 61–66
56. Megha, Sawatzki, P., Kolter, T., Bittman, R., and London, E. (2007) Effect of ceramide *N*-acyl chain and polar headgroup structure on the properties of ordered lipid domains (lipid rafts). *Biochim. Biophys. Acta* **1768,** 2205–2212
57. Nyholm, T. K., Grandell, P. M., Westerlund, B., and Slotte, J. P. (2010) Sterol affinity for bilayer membranes is affected by their ceramide content and the ceramide chain length. *Biochim. Biophys. Acta* **1798,** 1008–1013
58. Holopainen, J. M., Brockman, H. L., Brown, R. E., and Kinnunen, P. K. (2001) Interfacial interactions of ceramide with dimyristoylphosphatidylcholine. Impact of the *N*-acyl chain. *Biophys. J.* **80,** 1728–1738, 5321–5328.

J. Biol. Chem. **277,** 11788–11794
61. Cybulski, L. E., and de Mendoza, D. (2011) Bilayer hydrophobic thickness and integral membrane protein function. *Curr. Protein Pept. Sci.* **12,** 760–766
62. Ibarguren, M., Bomans, P. H., Frederik, P. M., Stonehouse, M., Vasil, A. I., Vasil, M. L., Alonso, A., and Goñi, F. M. (2010) End-products diacylglycerol and ceramide modulate membrane fusion induced by a phospholipase C/sphingomyelinase from *Pseudomonas aeruginosa*. *Biochim. Biophys. Acta* **1798,** 59–64
63. Nishio, M., Fukumoto, S., Furukawa, K., Ichimura, A., Miyazaki, H., Kusunoki, S., and Urano, T. (2004) Overexpressed GM1 suppresses nerve growth factor (NGF) signals by modulating the intracellular localization of NGF receptors and membrane fluidity in PC12 cells. *J. Biol. Chem.* **279,** 33368–33378